Available online at www.sciencedirect.com

ScienceDirect

Mendeleev Commun., 2022, **32**, 194–197

Mendeleev Communications

Synthesis and characterization of amantadinium iodoacetatobismuthate, a hybrid compound with mixed iodide–carboxylate anions

Tatiana A. Shestimerova,*[a] Mikhail A. Bykov,[a] Anastasia V. Grigorieva,[a,b] Zheng Wei,[c] Evgeny V. Dikarev[c] and Andrei V. Shevelkov[a]

[a] *Department of Chemistry, M. V. Lomonosov Moscow State University, 119991 Moscow, Russian Federation. E-mail: shestim@inorg.chem.msu.ru*

[b] *Department of Materials Sciences, M. V. Lomonosov Moscow State University, 119991 Moscow, Russian Federation*

[c] *Department of Chemistry, University at Albany, Albany, NY 12222, USA*

DOI: 10.1016/j.mencom.2022.03.014

The amantadinium iodoacetatobismuthate(III) $[C_{10}H_{15}NH_3 \cdot (CH_3)_2CO]_2[BiI_{3.67}(CH_3COO)_{1.33}]$ is a new hybrid halometallate with iodide ions partially replaced by oxygen-containing acetates to form stronger interaction between the anionic and cationic substructures. The title compound as well-shaped orange-red crystals was synthesized by a facile reaction in acetone solution in the presence of glacial acetic acid. The crystal structure of the compound consists of the infinite anionic chains $[BiI_{3.67}(CH_3COO)_{1.33}]^{2-}$ and the countercations $[C_{10}H_{15}NH_3 \cdot (CH_3)_2CO]^+$; according to the optical absorption data, the test compound is a semiconductor with a band gap of 2.06 eV.

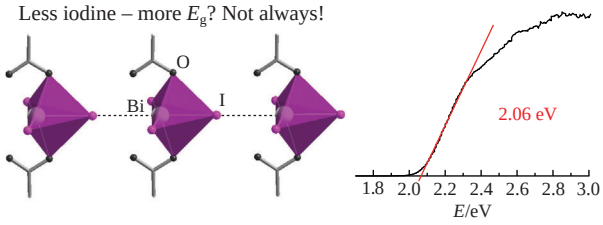

Keywords: amantadine, iodide, bismuth, acetate, perovskite photovoltaics.

The rapid development of perovskite photovoltaics has led to a significant increase in the research of halometallate compounds. Impressive progress in the efficiency of devices based on iodoplumbates from 3 to 27.9% has recently been achieved.[1–5] At the same time, the high toxicity of lead compounds requires the search for alternative hybrid light-harvesting halometallates.[6] The compounds of Bi^{3+} are promising candidates for the development of new light-harvesting materials for so-called perovskite solar cells. The bismuth cation exhibits an active $6s^2$ pair and strong spin-orbit coupling, and its low-toxicity compounds are stable towards oxidation and reduction. Although the current photovoltaic efficiency of solar cells based on bismuth cations is as low as 2.1%,[7–10] the studies of new compounds are oriented to provide better light-harvesting materials. In addition to potential photovoltaic properties, these compounds exhibit unusually diverse crystal structures and attractive luminescent and nonlinear optical characteristics.[11,12]

In diverse hybrid halobismuthates, the $[BiX_6]$ octahedra are principal building units. In various crystal structures, they share vertices, edges or faces leading to the formation of halobismuthate anions of different dimensionality with various organic cations as counterions. The composition and dimensionality of anions primarily affect the band gap, the second factor being additional binding by weak interactions between anions and cations. In general, upon going from chlorobismuthates to iodobismuthates and from 0D to 2D anions, the band gap narrows, whereas additional narrowing is provided by employing relatively strong N–H···I bonds and further by the inclusion of I_2 or I_3^- units.[13–20]

It is well known that the crystal structure and properties of halometallates can be altered by the partial replacement of halides by other anions such as thiocyanate or acetate.[21–23] For example, mixed-ligand $Cs_3Pb_2(CH_3COO)_2I_5$ is formed when the acetate anion partially substitutes for iodide in $CsPbI_3$.[22] Upon the substitution, the anionic substructure of parent 3D perovskite $\{PbI_3\}$ transforms into 1D ribbons $\{Pb_2(CH_3COO)_2I_5\}$, and the band gap increases from 1.73 to 2.57 eV, but strong phase-matching SHG response, large birefringence and high LDT properties arise. The disappearance of some properties along with the appearance of others and the possibility of constructing unusual crystal structures makes it attractive to study mixed-ligand iodometallates.

We consider an organic–inorganic hybrid with the formula $[C_{10}H_{15}NH_3 \cdot (CH_3)_2CO]_2[BiI_{3.67}(CH_3COO)_{1.33}]$ **1**, which is the first example of a mixed-ligand compound containing iodide and acetate anions in the coordination sphere of bismuth(III). Its red-orange crystals readily grow when a sample of bismuth(III) iodide and 1-aminoadamantane is dissolved in acetone, and glacial acetic acid is added to the solution.† The above formula of the compound was determined by single crystal X-ray diffraction analysis,‡ and the powder pattern calculated from the single crystal data was

† See Online Supplementary Materials for the synthesis procedures and detailed experimental data.

‡ *Crystal data for* **1**. $C_{28.67}H_{52}BiI_{3.67}N_2O_{4.67}$ (M = 1173.66), monoclinic, space group $C2$ at 100 K: a = 25.3763(10), b = 6.9424(3) and c = 10.8476(4) Å, Z = 2, d_{calc} =2.078 g cm^{-3}, V = 1875.99(13) Å^3, μ(MoKα) = 7.750 mm^{-1}, F(000) = 1105.3. A total of 17484 reflections were collected

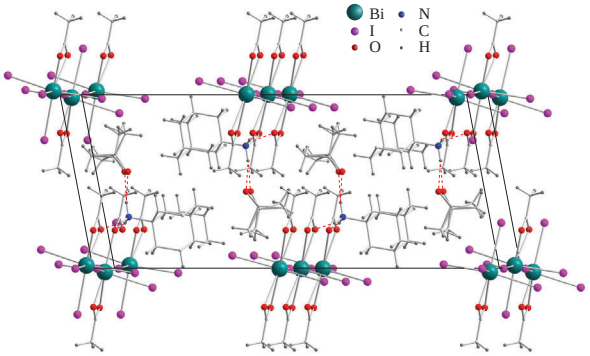

Figure 1 Crystal structure of compound **1**.

consistent with the experimental data obtained by powder X-ray diffraction analysis.

The crystal structure of compound **1** can be described as the $\{BiI_{3.667}(CH_3COO)_{1.333}\}^{2-}$ chains expanding along the *c* axis and $AdNH_3^+ \cdot (CH_3)_2CO$ cations, where $AdNH_3^+$ is the amantadinium cation $C_{10}H_{15}NH_3^+$ (Figure 1). The anionic chains $\{BiI_{3.667}(CH_3COO)_{1.333}\}^{2-}$ are essentially derived from the $\{BiI_5\}^{2-}$ chains built from corner-sharing $[BiI_6]$ octahedra. One-dimensional infinite linear $\{BiX_5\}^{2-}$ (X = Cl, Br and I) are quite rare, though there are several examples of bromobismuthates, mixed halides[23–32] and only two iodobismuthates.[27,33] Only one of those chains, $\{BiBr_5\}^{2-}$, is formed by slightly distorted octahedra,[31] while other halobismuthates usually exhibit heavy distortion of octahedral units so that the chain can be considered as stacks of tetragonal $[BiX_5]$ pyramids rather than a sequence of vertex-connected $\{BiX_6\}$ octahedra.[20–27,33,34] The anionic substructure of compound **1** is also formed by the stacks of pyramids, at the base of which acetate anions replace one or two iodides. A detailed structural, geometrical, and occupancy analysis shows that a pair of bismuth atomic positions can be clearly distinguished in the structure: Bi(1) and Bi(2), which form two $\{BiI_4(CH_3COO)\}$ and $\{BiI_3(CH_3COO)_2\}$ chains, respectively, alternating in a ratio of 1:2 in the crystal

Table 1 Important bonding distances in the crystal structure of compound **1** with two types of chains.[a]

Chain $\{BiI_4(CH_3COO)\}$		Chain $\{BiI_3(CH_3COO)_2\}$	
Bond	Bond length/Å	Bond	Bond length/Å
Bi(1)–I(1)	3.164(5)	Bi(2)–I(1)^{ii}	3.006(3)
Bi(1)–I(1)^{ii}	3.792(6)	Bi(2)–I(1)	3.936(4)
Bi(1)–I(2)	3.076(9)	Bi(2)–I(31)	3.010(4)
Bi(1)–I(31)^{i}	3.046(12)	Bi(2)–I(32)	3.075(4)
Bi(1)–I(32)	3.016(11)	Bi(2)–O(32)*2	2.503(19)
Bi(1)–O(33)^{i}*2	2.38(2)		
Bi(1)–O(32)	2.644(19)		

[a] Symmetry codes: (i) $-x + 1, y, -z + 2$; (ii) $x, y - 1, z$.

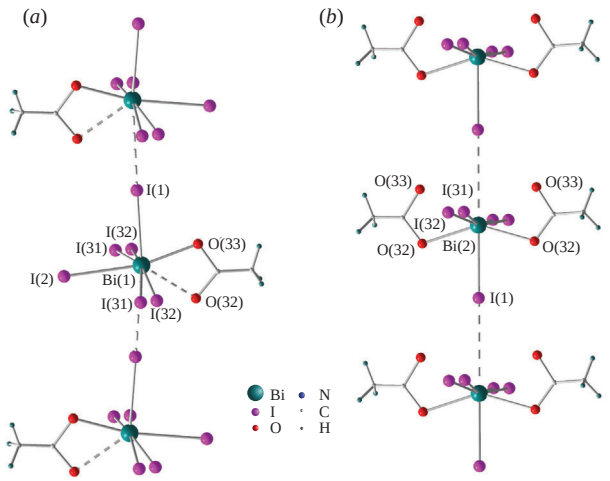

Figure 2 Two types of chains in the crystal structure of compound **1**: (*a*) $\{BiI_4(CH_3COO)\}$ and (*b*) $\{BiI_3(CH_3COO)_2\}$. Note that the I(31) and I(32) atoms are disordered: the I(31)–I(32) distance between the adjacent atoms is 0.66 Å.

structure. The Bi(1) atom forms $\{BiI_4(CH_3COO)\}$ chains, and its ligand environment can be considered as five iodine atoms at a distance of 3.01–3.16 Å (Table 1), with one of the two I(2) atoms being replaced by an acetate ion. The bismuth–oxygen bond lengths of 2.38 and 2.64 Å for Bi(1)–O(33) and Bi(1)–O(32), respectively, are common for bismuth carboxylates.[35] The square pyramidal environment of the bismuth atom is supplemented by the Bi(1)–I(1) contact of 3.79 Å [Figure 2(*a*)]. The Bi(2) atom forms $\{BiI_3(CH_3COO)_2\}$ chains [Figure 2(*b*)], and it is bound to three iodine atoms at distances of 3.00–3.08 Å and to two monodentate carboxylates at a distance of 2.50 Å, which was observed in various bismuth oxo compounds.[36] The longest Bi(2)–I(1) distance in the coordination sphere of Bi(2) is 3.94 Å. This distance is too long to be a covalent bond; however, such distances were reported for the crystal structure of Ni_8Bi_8SI.[37]

Unlike viologen halobismuthates, there are strong hydrogen bonds between the cation and the anion in compound **1**. All hydrogen

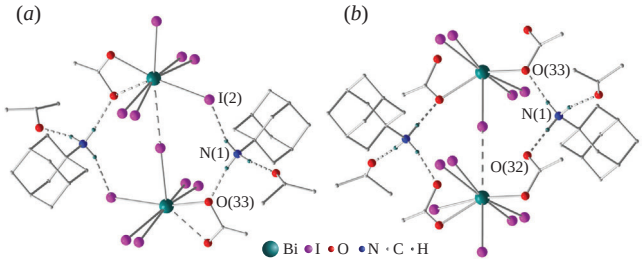

Figure 3 Weak interactions in the crystal structure of compound **1** with two types of chains: (*a*) $\{BiI_4(CH_3COO)\}$ and (*b*) $\{BiI_3(CH_3COO)_2\}$. Hydrogen atoms of the adamantane cage are omitted for clarity.

(3446 independent reflections, $R_{int} = 0.0602$), GOF = 1.079, final refinement parameters *R* indices [$I > 2\sigma(I)$]: $R_1 = 0.0536$ and $wR_2 = 0.0721$, *R* indices (all data) $R_1 = 0.0816$ and $wR_2 = 0.0792$, 173 restrains and 233 refined parameters; largest diff. peak/hole 1.146/–1.416 e Å^{-3}. The single crystal diffraction data were measured at 100(2) K on a Bruker D8 VENTURE with a PHOTON 100 CMOS detector system and a graphite monochromator equipped with a Mo-target X-ray tube. Frame width of 0.50° and an exposure time of 15 s frame^{-1} were employed for the data collection. Data reduction and integration were performed with the Bruker software package SAINT (Version 8.38A).[24] Data were corrected for absorption effects using the semi-empirical methods (multi-scan) implemented in SADABS (Version 2014/5).[25] The crystal structure was solved by direct methods using the SHELXTL (Version 2018/3) program package,[26] which gave positions of bismuth and iodine atoms. There was a reduced occupation and unrealistic thermal parameters for I(2) atoms and the Bi positions splitting. Difference Fourier syntheses gave the positions of nitrogen and carbon atoms of amantadinium cations and acetone molecules and showed three additional peaks near the I(2) atom. When the partial substitution of I(2) atoms by acetate groups was checked, that led to a significant decrease in *R* factor values. Various options for splitting bismuth atomic positions and refinement of the occupancies of iodine and acetate groups positions were tried; as a result, a model with two types of chains was proposed. Hydrogen atoms were calculated and further refined using the riding model. In the final step, the crystal structure was refined with anisotropic approximations of atomic displacement parameters for all non-hydrogen atoms.

CCDC 2089678 contains the supplementary crystallographic data for this paper. These data can be obtained free of charge from The Cambridge Crystallographic Data Centre *via* http://www.ccdc.cam.ac.uk.

Table 2 Hydrogen bonding in the crystal structure of compound **1**.[a]

D–H···A	*d*(H···A)/Å	*d*(D···A)/Å	∠(D–H···A)/deg
N(1)–H(1B)···O(1AC)	1.879	2.786	174.53
N(1)–H(1B)···O(1AD)	1.941	2.833	166.13
N(1)–H(1A)···I(2)^{i}	2.925	3.768	154.73
N(1)–H(1A)···O(33)^{ii}	1.893	2.788	167.65
N(1)–H(1C)···O(32)	1.930	2.830	169.70

[a] Symmetry codes: (i) *x*, *y* – 1, *z*; (ii) –*x* + 1, *y* – 1, –*z* + 2.

atoms of the ammonium group in the amantadinium cation participate in the formation of hydrogen bonds (Figure 3). Two of them connect neighboring tetragonal pyramids either through the N–H···O interaction with the acetate group and the N–H···I contact with iodine or through two N–H···O bonds with the acetate group. In both cases, the third hydrogen atom restrains the solvent acetone molecule due to the N–H···O interaction of 1.9 Å (Table 2). Strong N–H···O hydrogen bonds between the NH_3 group and the acetone oxygen allowed us to consider the cationic substructure as $[C_{10}H_{15}NH_3{\cdot}(CH_3)_2CO]^+$. It is well known that solvent molecules can participate in the cationic substructure and affect the assembly and crystallization of halometallate hybrids.[38,39]

Usually, acetone-containing compounds are extremely unstable in air.[40] Thermogravimetric analysis shows that compound **1** is sufficiently stable due to the formation of strong hydrogen bonds, and the removal of acetone starts only at 114 °C. Further decomposition can be described as the successive loss of two acetone molecules followed by 1.3 molecules of aminoadamantane acetate and, finally, 0.7 molecules of HI.

The Raman spectrum of compound **1** (Figure 4) exhibits a strong and broad asymmetric peak at 127 cm^{-1}, which can be assigned to different Bi–I bonds by analogy to other iodobismuthates, which show Raman shifts between 100 and 145 cm^{-1}.[13,42–44] The lower Raman shift observed at 83 cm^{-1} can be assigned to bending modes and to N–H···O or N–H···I hydrogen bonds (see Table 2), although an unambiguous assignment of this peak is hardly possible because of the expected overlap of various contributions. At higher Raman shifts in a range of 400–1600 cm^{-1}, bands of valence and deformation vibrations of C–N and C–H bonds in the amantadinium cation and the acetate anion are observed; a detailed assignment of the vibration frequencies is given in Table S2, see Online Supplementary Materials. Compound **1** exhibits the valence vibration of the C=O bond of acetone near 1690 cm^{-1}. Its shift to the lower frequency, as compared to the valence vibrations of the C=O group in a free acetone molecule (1720–1740 cm^{-1}), is associated with the C=O···H–N hydrogen bond between the amantadinium cation and the acetone molecule (see Figure 3).

Compound **1** is red-orange, and this color nicely correlates with the band gap found from the UV-VIS optical absorption: the Kubelka–Munk conversion results in E_g = 2.06 eV (Figure 5). This value is comparable to that of pure iodobismuthates with

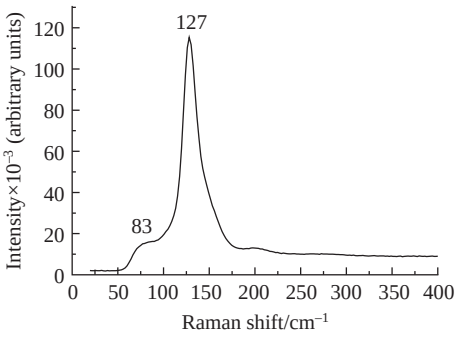

Figure 4 Low-shift part of the Raman spectrum of compound **1**.

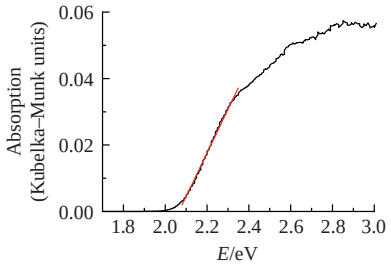

Figure 5 Kubelka–Munk plot for compound **1**.

BiI_5^{2-} zigzag chains[13,44] and somewhat higher than that of pure viologen iodobismuthates with linear chains (1.7 eV).[33,34] It is assumed that the band gap is mainly determined by the structure of the anion and almost independent of the cation.[17,41] Usually, the replacement of iodine atoms in the anion with other ligands leads to the band gap widening.[27,28] In compound **1**, the band gap does not increase as much as one would expect. The reasons are unclear, and we can only assume that weak cation–anion interactions like N–H···O or N–H···I play a role similar to that in cases when such interactions facilitated band gap narrowing.[20,21]

In conclusion, despite a heavy disorder in the crystal structure, the test compound can be properly described as comprising of $\{BiI_3(CH_3COO)_2\}$ and $\{BiI_4(CH_3COO)\}$ chains randomly distributed in the structure in a ratio of 1:2 and $[C_{10}H_{15}NH_3{\cdot}(CH_3)_2CO]^+$ cations with strong N–H···O bonds between the NH_3 group and the acetone oxygen. Additional hydrogen bonds link the cation through its NH_3 group with iodine or acetate oxygen atoms of the ligands bound to bismuth atoms to provide reasonable thermal stability of compound **1** and a band gap of 2.06 eV. We assume that mixing anions is an attractive approach to tailoring the band gap of halometallates along with controlling the dimensionality of the anionic part, introducing polyhalide moieties and employing weak interactions.

This work was supported by the Russian Foundation for Basic Research (grant no. 20-03-00280). Z.W. and E.V.D. thank the National Science Foundation (grant no. CHE-1955585) for supporting structural studies.

Online Supplementary Materials

Supplementary data associated with this article can be found in the online version at doi: 10.1016/j.mencom.2022.03.014.

References

1 K. Lin, J. Xing, L. N. Quan, F. P. G. de Arquer, X. Gong, J. Lu, L. Xie, W. Zhao, D. Zhang, C. Yan, W. Li, X. Liu, Y. Lu, J. Kirman, E. H. Sargent, Q. Xiong and Z. Wei, *Nature*, 2018, **562**, 245.
2 Y. Shen, L.-P. Cheng, Y.-Q. Li, W. Li, J.-D. Chen, S.-T. Lee and J.-X. Tang, *Adv. Mater.*, 2019, **31**, 1901517.
3 Y. Cao, N. Wang, H. Tian, J. Guo, Y. Wei, H. Chen, Y. Miao, W. Zou, K. Pan, Y. He, H. Cao, Y. Ke, M. Xu, Y. Wang, M. Yang, K. Du, Z. Fu, D. Kong, D. Dai, Y. Jin, G. Li, H. Li, Q. Peng, J. Wang and W. Huang, *Nature*, 2018, **562**, 249.
4 F. Sahli, J. Werner, B. A. Kamino, M. Bräuninger, R. Monnard, B. Paviet-Salomon, L. Barraud, L. Ding, J. J. Diaz Leon, D. Sacchetto, G. Cattaneo, M. Despeisse, M. Boccard, S. Nicolay, Q. Jeangros, B. Niesen and C. Ballif, *Nat. Mater.*, 2018, **17**, 820.
5 E. Köhnen, P. Wagner, F. Lang, A. Cruz, B. Li, M. Roß, M. Jošt, A. B. Morales-Vilches, M. Topič, M. Stolterfoht, D. Neher, L. Korte, B. Rech, R. Schlatmann, B. Stannowski and S. Albrecht, *Sol. RRL*, 2021, **5**, 2100244.
6 F. Cao and L. Li, *Adv. Funct. Mater.*, 2021, **31**, 2008275.
7 T. Li, Y. Hu, C. A. Morrison, W. Wu, H. Hana and N. Robertson, *Sustainable Energy Fuels*, 2017, **1**, 308.
8 J. Zhang, S. Han, C. Ji, W. Zhang, Y. Wang, K. Tao, Z. Sun and J. Luo, *Chem. – Eur. J.*, 2017, **23**, 17304.

9 Z. Zhang, X. Li, X. Xia, Z. Wang, Z. Huang, B. Lei and Y. Gao, *J. Phys. Chem. Lett.*, 2017, **8**, 4300.
10 A. N. Usoltsev, M. Elshobaki, S. A. Adonin, L. A. Frolova, T. Derzhavskaya, P. A. Abramov, D. V. Anokhin, I. V. Korolkov, S. Yu. Luchkin, N. N. Dremova, K. J. Stevenson, M. N. Sokolov, V. P. Fedin and P. A. Troshin, *J. Mater. Chem. A*, 2019, **7**, 5957.
11 S. A. Adonin, M. N. Sokolov and V. P. Fedin, *Coord. Chem. Rev.*, 2016, **312**, 1.
12 S. A. Adonin, M. N. Sokolov and V. P. Fedin, *Coord. Chem. Rev.*, 2018, **367**, 1.
13 T. A. Shestimerova, A. V. Mironov, M. A. Bykov, E. D. Starichenkova, A. N. Kuznetsov, A. V. Grigorieva and A. V. Shevelkov, *Cryst. Growth Des.*, 2020, **20**, 87.
14 T. A. Shestimerova, N. A. Golubev, N. A. Yelavik, M. A. Bykov, A. V. Grigorieva, Z. Wei, E. V. Dikarev and A. V. Shevelkov, *Cryst. Growth Des.*, 2018, **18**, 2572.
15 V. Yu. Kotov, A. B. Ilyukhin, A. A. Sadovnikov, K. P. Birin, N. P. Simonenko, H. T. Nguyen, A. E. Baranchikov and S. A. Kozyukhin, *Mendeleev Commun.*, 2017, **27**, 271.
16 P. Liebing, F. Stein, L. Hilfert, V. Lorenz, K. Oliynyk and F. T. Edelmann, *Z. Anorg. Allg. Chem.*, 2019, **645**, 36.
17 A. J. Dennington and M. T. Weller, *Dalton Trans.*, 2016, **45**, 17974.
18 S. A. Adonin, I. D. Gorokh, A. S. Novikov, D. G. Samsonenko, I. V. Yushina, M. N. Sokolov and V. P. Fedin, *CrystEngComm*, 2018, **20**, 7766.
19 T. Li, Q. Wang, G. S. Nichol, C. A. Morrison, H. Han, Y. Hu and N. Robertson, *Dalton Trans.*, 2018, **47**, 7050.
20 T. A. Shestimerova, A. V. Mironov, M. A. Bykov, A. V. Grigorieva, Z. Wei, E. V. Dikarev and A. V. Shevelkov, *Molecules*, 2020, **25**, 2765.
21 T. A. Shestimerova, N. A. Golubev, A. V. Grigorieva, M. A. Bykov, Z. Wei, E. V. Dikarev and A. V. Shevelkov, *Russ. Chem. Bull.*, 2021, **70**, 39.
22 Q.-R. Shui, H.-X. Tang, R.-B. Fu, Y.-B. Fang, Z.-J. Ma and X.-T. Wu, *Angew. Chem., Int. Ed.*, 2021, **60**, 2116.
23 M. Daub and H. Hillebrecht, *Angew. Chem., Int. Ed.*, 2015, **54**, 11016.
24 *SAINT, Data Reduction and Correction Program, version 8.38A*, Bruker AXS, Madison, WI, 2017.
25 L. Krause, R. Herbst-Irmer, G. M. Sheldrick and D. Stalke, *J. Appl. Crystallogr.*, 2015, **48**, 3.
26 G. M. Sheldrick, *Acta Crystallogr., Sect. C: Struct. Chem.*, 2015, **71**, 3.
27 N. Leblanc, N. Mercier, M. Allain, O. Toma, P. Auban-Senzier and C. Pasquier, *J. Solid State Chem.*, 2012, **195**, 140.
28 N. Leblanc, N. Mercier, L. Zorina, S. Simonov, P. Auban-Senzier and C. Pasquier, *J. Am. Chem. Soc.*, 2011, **133**, 14924.
29 M. Owczarek, P. Szklarz, R. Jakubas and A. Miniewicz, *Dalton Trans.*, 2012, **41**, 7285.
30 W. Bi, N. Leblanc, N. Mercier, P. Auban-Senzier and C. Pasquier, *Chem. Mater.*, 2009, **21**, 4099.
31 S. A. Adonin, I. D. Gorokh, A. S. Novikov, P. A. Abramov, M. N. Sokolov and V. P. Fedin, *Chem. – Eur. J.*, 2017, **23**, 15612.
32 V. Yu. Kotov, A. B. Ilyukhin, P. A. Buikin and K. E. Yorov, *Mendeleev Commun.*, 2019, **29**, 537.
33 Y. Chen, Z. Yang, C.-X. Guo, C.-Y. Ni, Z.-G. Ren, H.-X. Li and J.-P. Lang, *Eur. J. Inorg. Chem.*, 2010, 5326.
34 V. Yu. Kotov, A. B. Ilyukhin, A. A. Korlyukov, A. F. Smol'yakov and S. A. Kozyukhin, *New J. Chem.*, 2018, **42**, 6354.
35 C.-I. Stålhandske, *Acta Chem. Scand.*, 1969, **23**, 1525.
36 A. W. Kelly, A. M. Wheaton, A. D. Nicholas, H. H. Patterson and R. D. Pike, *J. Inorg. Organomet. Polym. Mater.*, 2008, **28**, 528.
37 A. I. Baranov, L. Kloo, A. V. Olenev, B. A. Popovkin, A. I. Romanenko and A. V. Shevelkov, *J. Am. Chem. Soc.*, 2001, **123**, 12375.
38 T. Yu, J. Shen, Y. Wang and Y. Fu, *Eur. J. Inorg. Chem.*, 2015, 1989.
39 T. Yu, H. Li, P. Hao, J. Shen and Y. Fu, *Eur. J. Inorg. Chem.*, 2016, 4878.
40 S. A. Adonin, E. V. Peresypkina, M. N. Sokolov and V. P. Fedin, *Russ. J. Coord. Chem.*, 2014, **40**, 867 (*Koord. Khim.*, 2014, **40**, 699).
41 N. A. Yelovik, A. V. Mironov, M. A. Bykov, A. N. Kuznetsov, A. V. Grigorieva, Z. Wei, E. V. Dikarev and A. V. Shevelkov, *Inorg. Chem.*, 2016, **55**, 4132.
42 C. Hrizi, A. Samet, Y. Abid, S. Chaabouni, M. Fliyou and A. Koumina, *J. Mol. Struct.*, 2011, **992**, 96.
43 J. Laane and P. W. Jagodzinski, *Inorg. Chem.*, 1980, **19**, 44.
44 G. A. Mousdis, G. C. Papavassiliou, A. Terzis and C. P. Raptopoulou, *Z. Naturforsch., B: J. Chem. Sci.*, 1998, **53**, 927.

Received: 28th July 2021; Com. 21/6626